Bead Coating Instability: A Comparison of Speed Limit Data with Theory

JOHN A. TALLMADGE
CHARLES B. WEINBERGER
and
HELEN L. FAUST

Department of Chemical Engineering
Drexel University
Philadelphia, Pennsylvania 19104

Bead coating geometry is used in the continuous, high-speed coating of photographic and other films. However, bead coating suffers from instabilities occurring at maximum and minimum speeds which result in nonuniform films and unsatisfactory coating. This article describes an experimental study of these speeds for a range of flowrates, gaps, and viscosities. Results are compared with theory.

SCOPE

As with most coating processes, bead coating is limited to certain speed ranges by flow, geometry, and fluid properties. We report here an experimental study of bead coating for three viscous liquids, having viscosities of 22 to 281 mN·s/m^2, for the case of a zero pressure difference across the bead. The influence of a four-fold range of gap size (0.5 to 2.0 mm) and a three-fold range of volume flowrate (150 to 450 ml/min) for a wide range of coating speeds (7 to 50 m/min) are studied, using a constant slide width of 25.4 mm. Results are compared with predictions from a theoretical model developed by Ruschak (1976).

CONCLUSIONS AND SIGNIFICANCE

Upper and lower speed limits are observed for given settings of volume flowrate, gap size, and liquid viscosity. These limits are given here, based on the "split point" for the upper limit and the "drip point" for the lower limit. Over the ranges studied, both speed limits are found to vary approximately with the + 0.8 power of flowrate, the −0.3 power of viscosity, and the + 0.1 power of gap size. An important, though unexpected, result is the observation that the lower speed limit exhibited approximately the same dependence on these process variables as the upper speed limit.

The upper speed limit effects predicted by the Ruschak model agreed, in general, for flowrate (+ 0.6 power) and viscosity (−0.4 power), but did not agree in terms of gap size (−0.6 power). The effect of gap size deserves further study, but the effects of flowrate and viscosity on the upper limit seem to be reasonably well described by data and theory. The observed lower speed limit is not predicted by the Ruschak model for the case of a zero pressure difference, probably because the lower meniscus was approximated as quasi-static in the model.

A brief study of the flow pattern in the bead, at one set of conditions, indicates that no vortices were present. The effect of coating speed on bead size and shape, reported for a constant gap size (1.0 mm) and a high flowrate, indicates a large effect on the upper meniscus and a small effect on the lower meniscus.

Included in this article, therefore, are methods for studying bead and menisci sizes of large beads and for studying both upper and lower speed limits of viscous liquids. Speed limit data are also reported and compared with theory for a range of flowrates, gap sizes, and viscosities.

INTRODUCTION

An object can be coated with a liquid by withdrawing the object from a pool of the liquid. This process, often called dip coating, has the disadvantage that the resultant film thickness is determined by withdrawal speed and fluid properties in a complex way. Therefore, obtaining the desired film thickness and minimizing thickness variation both are difficult problems.

Pre-metered coating techniques do not have this disadvantage. One important commercial method of premetered coating is bead coating. This involves metered flow of a liquid through a slot in an applicator, down a slide, across a gap, and then onto a flat surface moving at a constant speed; the process is sometimes called slide coating. Bead coating has been described in several patents, Beguin (1954), for example. As with most types of coating processes, bead coating is limited at some high speed by an instability. Description of the influence of variables on speed limits in continuous bead coating is one of our purposes here.

In the first half of this decade, Faust (1975) conducted an experimental study of bead coating stability limits in our laboratory. This study included determination of speed limits for several Newtonian liquids with different viscosities, over a range of volume flowrates and gap sizes. Ruschak (1976), in a theoretical study of the problem, derived predictive equations for similar speed limits in a pre-metered coating device. In this article, the speed limits of Faust will be presented, discussed, and compared with the published theory of Ruschak.

GEOMETRY

Liquid, at a metered volumetric flowrate Q, flows down a slide of width b, forms a bead across a gap space of distance d, and is entrained by a flat belt surface moving vertically at a speed s (see Figure 1). The liquid properties of density ρ, viscosity μ, and surface tension σ are uniform. Above the bead the entrained liquid thickness h (from the belt) approaches a constant film thickness h_a asymptotically. An angle α is formed between the slide and the normal to the moving belt.

0001-1541-79-1925-1064-$01.00.

For a given metered flowrate Q and a constant speed s, the resultant film thickness, if spread over a width b, will be given by

$$h_a = Q/(sb) \qquad (1)$$

Because of Equation 1, setting and obtaining the desired film thickness is not a problem for bead coating. However, obtaining a uniform or stable film requires selection of belt speeds within range of "operable" limits.

APPARATUS

A continuous belt apparatus, shown in Figure 2, is used for the coating experiments. It is modified for bead coating from a belt apparatus assembled by Soroka (1969), who used the method and belts of Gutfinger and Tallmadge (1964). While the major aspects of the apparatus are described here, other details are given in thesis form (Faust 1975).

The belt is 62 mm wide, 0.15 mm thick, and about 2,500 mm long. It is made of an endless stainless steel sheet positioned between two 0.14 m ID pulleys with a center distance of 0.99 m. The upper pulley is driven by a precision, variable-speed motor. A galvanized steel slide (or trough) was built to transfer liquid to the moving belt. The slide is 25.4 mm wide, with 13 mm high sides, beveled at the gap end, and 0.60 m long. The slide is positioned 0.29 m above the center of the bottom pulley and tilted so that the angle α is approximately 45°. The gap between the slide and the belt was measured with the gap space micrometer, positioned centrally and just below the bottom edge of the slide and sensitive to 1 μm. The gap is set at the beginning of each run sequence, while the melt is moving, and rechecked at the end of each sequence. The slide is purposely made narrower than the belt, to eliminate edge effects on the side of the belt.

The liquids are metered from a reservoir to the slide, using a valve and a variable-area rotameter. A constant-head tank, having a capacity of 0.019 m^3, (5 gal.) is used to provide a uniform, gravity-driven flow. A centrifugal pump is used to raise the liquid from the feed tank reservoir to the head tank. Spring-loaded wipers on both sides of the belt remove the coating liquid. The front and back wipers both are at the same height, about 0.25 m below the center of the top pulley. The wipers are wider than the belt to ensure complete wiping and also are angled downward to facilitate transfer of the wiped fluid into the return trough.

All tests are made in a constant temperature room, with the temperature recorded on each test day. The room temperature air is 19 ± 1°C for two-thirds of the 32 sets of runs. Thermometers in the feed tank and the return line monitored the liquid temperature.

The film thickness h_a was measured with a micrometer with a custom-made tip, placed at the horizontal center of the film, about 0.57 m above the center of the bottom pulley. The micrometer contact point is determined using the visual method of Soroka-Gutfinger. Film thickness is then calculated by subtracting the thickness of the dry belt. This visual method was developed by Gutfinger (1964) and noted in Gutfinger and Tallmadge (1964). The design of the micrometer was improved by Soroka (1969).

LIQUIDS USED

The first liquid studied is a glycerin-water solution with 75 weight % glycerin, coded as fluid G. The viscosity of this solution, 22 mN·s/m^2 (22 cp), is sufficient to provide bead and film thicknesses of appreciable size, as described here. Two other liquids tested are oils of higher viscosity, namely a paraffin oil of 68 mN·s/m^2, coded fluid P, and a oil mixture of 281 mN·s/m^2, coded fluid M. The oil mixture is prepared by mixing one part of a paraffin oil with two parts of a motor oil, by volume.

These three Newtonian fluids provide a thirteen-fold range of viscosities. The glycerin solution is used to simulate actual bead coating operation. The two oils were also selected to provide larger beads and, consequently, larger meniscus profiles.

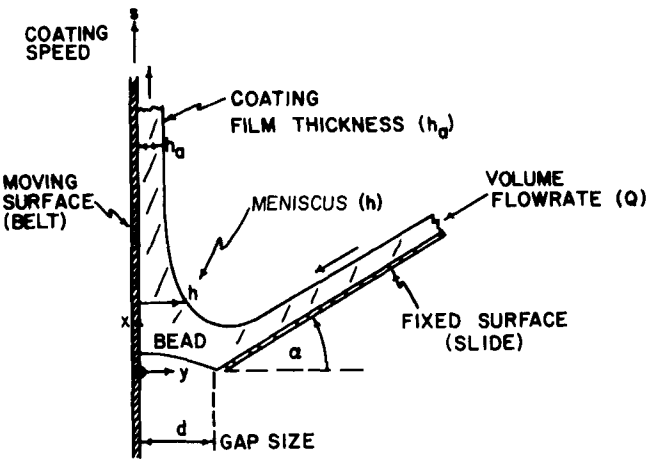

Figure 1. Schematic drawing of bead coating.

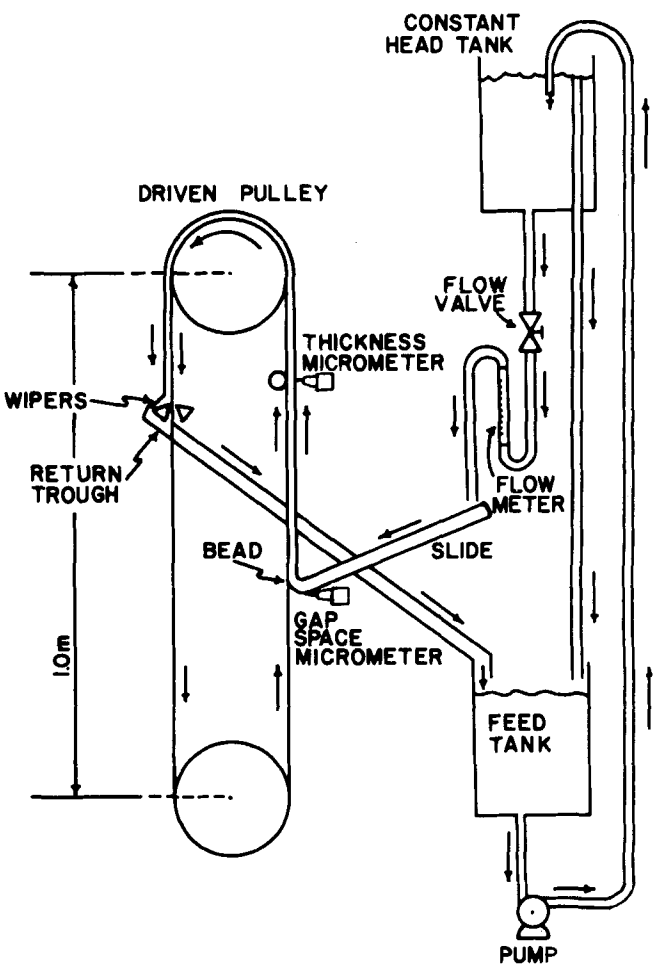

Figure 2. Bead coating apparatus.

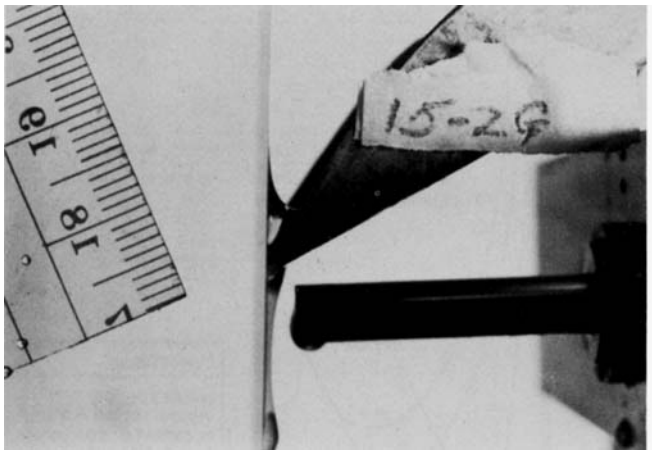

Figure 3A. Drip point in bead coating (13.9 m/min speed, 1.0 mm gap, 160 ml/min flowrate, glycerin run 152G.)

Figure 3B. Split point in bead coating (19.2 m/min speed, 1.0 mm gap, 160 ml/min flowrate, glycerin run 156G).

The surface tensions of the three liquids G, P, and M are similar: 39.4, 34.1, and 33.6 N/km (or dyne/cm), respectively. Densities for the same liquids are 1,180, 865, and 902 kg/m^3, respectively. Viscosity is measured by standard Cannon-Fenske, falling-level capillary viscometers, with variations less than 1%. Density is measured with hydrometers accurate to within 0.2%. Surface tension is measured with a ring tensiometer, the Fisher Tensiomat Model 21, with variation of 0.5%. These fluid properties were measured in a constant temperature room with an air temperature which was usually within one degree of 19°C.

Small increase in return-line, liquid temperatures were noted in some preliminary run sequences. These small changes are due primarily to viscous heating in the pump and lines; heating from the photo illuminating lamp is believed to be secondary or negligible. Since the increase in liquid temperature has a tendency to influence other fluid properties, the viscosity of the liquid is measured twice for each run sequence, at the beginning and end, and averaged. The absolute variation in viscosity (due to temperature changes in a run sequence) is no more than 0.002 Ns/m^2 for glycerine and paraffin sequences. Thus the relative variation for paraffin runs is 3% or less, but up to 10% for the glycerin runs. Most of the temperature increases were noted with the higher viscosity oils, particularly the motor oil mixture.

PROCEDURE AND EFFECT OF BELT SPEED

To obtain a general description of measurement techniques and the range of variables (such as operable speed ranges, bead sizes, and meniscus profiles), 13 preliminary sets of runs are made with the glycerin solutions. Based on these tests, we decided to vary gap distance from 0.5 to 1.5 mm and liquid flowrates from 150 to 450 ml/min for the glycerin solutions. For these ranges of gaps and flows, the resulting belt speeds studied with glycerin solutions are 13 to 50 m/min, (about 0.7 to 2.7 fps).

The belt speed is controlled by setting the potentiometer for the motor drive and was determined for each run by measuring the number of revolutions of the top pulley in one minute. This works well, because the speed is very constant during continuous operation, such as during a run sequence.

The day-to-day speed fluctuation in the belt speed for the same potentiometer setting which occurs (Soroka 1969) is avoided by measuring speed during each run. At a potentiometer reading of 110, for example, the day-to-day speeds are in the range of 7.2 ± 0.5 m/min (or ± 7%). Because the absolute variations here are fairly constant, the relative size of these ranges are smaller at higher speeds.

In this work, speed is varied to seek uniform films, while holding viscosity, gap size, and flowrate constant. For example, consider a typical set of conditions, namely glycerin solution at a 1.5 mm gap and 240 ml/min flowrate.

First, in preliminary tests, the belt speed potentiometer (or pot) is slowly varied up and down. Observing both the bead and the film indicates that nonuniformities appeared at pot readings of 345 and lower, as well as 450 and higher (the respective speeds were 20.8 and 26.1 m/min). More importantly, the film is quite uniform at all intermediate speeds. These and other similar tests show that it is necessary to maintain a stable bead to obtain a uniform film.

With this information, a sequence of runs was made, set 27 in this case. Here the belt speed is reduced and set at the lower speed limit (pot 345), a run taken, and then the speed increased at finite increments for subsequent runs. For each run, a photograph of the bead is made, the film thickness measured, and visual observations concerning the type of film are recorded.

Results and conditions for this sequence of runs are shown in Table 1. The first two numbers in the run number code are the sequence number at constant gap and flow, and the third designates the specific speed. Table 1 indicates the speed steps chosen and the double checks with thickness, but the most important result is the type of film. The film type is used to select the upper and lower speed limits for uniformity and, therefore, the limits for instability.

The lower limit of the speed range is defined to be that speed equal to the "drip point," 20.8 m/min in this case. The drip point is that speed, when slowly decreased, at which the bead becomes too large to be maintained in the gap, and instability first occurs. Fluid tends to drip down the belt below the point of application. The speed just above the drip point is the lowest operable speed for a stable, uniform film (here, 21.1 m/min). The bead (at this lowest operable point) is the largest that may be maintained at the given conditions of fluid flowrate, gap space, and fluid viscosity. For this reason, the lower operable speed is called the "fat bead" point by Faust (1975). Because the two points noted above are difficult to obtain with discrete speed tests, the lower speed limit is given here as a range, 20.8 to 21.1 m/min. At the drip

Table 1. Experimental Method for Range of Speeds (a,b)

Run No. (c)	Belt speed Pot.	Belt speed m/min.	Film thicknesses, h_a, in microns: Measured	Calc(d)	Diff.	Type of film
271	345	20.8	—	—	—	Drip
272	350	21.1	46.3	44.8	−3.2%	Uniform
273	375	22.0	40.3	42.9	+6.5%	Uniform
274	400	24.0	39.7	39.5	−0.5%	Uniform
275	425	24.9	38.7	37.9	−2.1%	Uniform
276	435	25.4	37.4	36.2	−3.2%	Uniform
277	450	26.1	—	—	—	Split

(a) With glycerin solution G, viscosity of 22 mN.s/m² (22 cp).
(b) With 1.5 mm gap and 240 ml/min flowrate.
(c) Run sequence 27.
(d) Calculated from volume flowrate using Equation (1).

point, the drip is often quite pronounced, as shown photographically in Figure 3A. This picture was taken with glycerin at another set of conditions.

The upper limit of the speed range is defined as that speed equal to the "split point," 26.1 m/min here. The split point is that speed at which the amount of fluid bridging the gap space is less than that needed to maintain a bead and a uniform film. Three types of high-speed non-uniformities were observed in the many sequences studied. In one, the film splits into two or more individual streams; in another the film becomes very narrow and does not form a uniform film coating; in the third, the film is not able to bridge the gap space and runs off the end of the slide without touching the belt. The most common occurrence is the split of the film into two distinct streams (Figure 3B). It is the belt speed just below this unstable, split-point speed that sets the upper operable speed. The bead at this highest operable speed is the smallest that may be maintained at the given conditions, so for this reason, the upper speed range limit is called the "thin bead." The upper speed limit is given as a range, 25.4 to 26.1 m/min in this case.

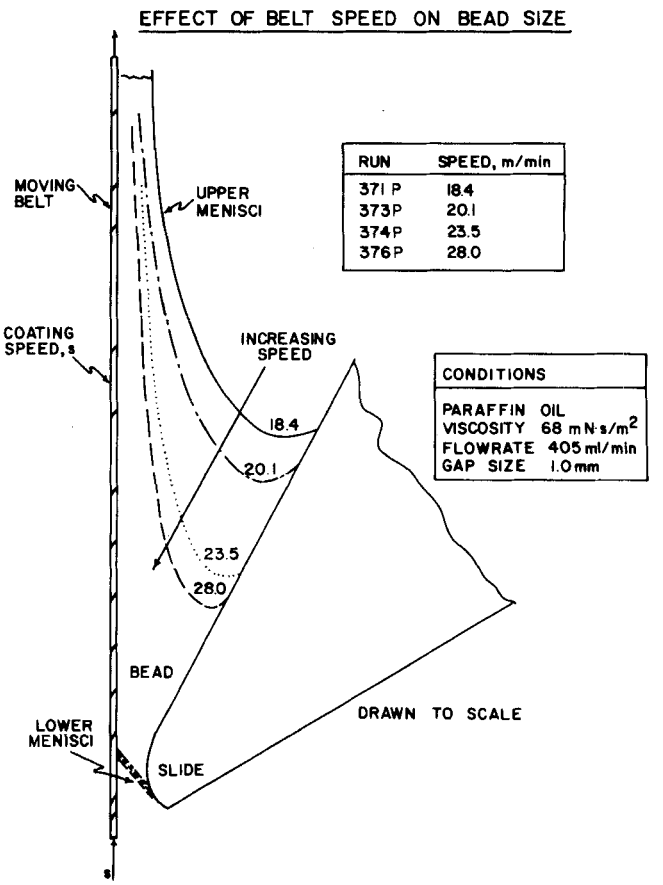

Figure 4. Bead sizes with paraffin oil.

In summary, the operable range of the coating speeds lies within the drip point and split point. The operable range for sequence 27 conditions is about 21 to 26 m/min.

Table 2. Run Conditions and Speed Limits for Glycerin (b)

Flowrate Q, ml/min	Size of gap, mm	Run Nos. (c)	Liquid prop. air: μ, cp	T°C	T°C	Range of speed limits, m/min: Upper speed (split)	Lower speed (drip) (d)
155	0.5	235-6	20	26	21	18.9-20.3	13.6-14.6
155(a1)	1.0	154-6	28	22	19	18.0-19.2(a1)	13.9-14.8
155(a1)	1.0	216-7	19	26	22	17.7-18.9(a1)	15.3-15.8
156	1.5	175-6	25	21	19	16.5-19.4	13.9-14.4
260	0.5	247-8	22	25	20	25.9-26.4	20.6-21.1
240	1.0	146-7	26	26	19	28.2-32.6	21.6-23.7
250(a2)	1.5	185-6	24	22	17	24.9-26.3(a2)	22.0-22.5
255(a2)	1.5	208-9	20	25	22	31.6-32.6(a2)	22.0-24.7
240(a2)	1.5	276-7	22	23	18	25.4-26.1(a2)	20.8-21.1
405	0.5	257-8	22	23	19	37.4-38.8	30.7-31.4
450(a3)	1.0	168-9	22	24	20	38.3-39.8(a3)	28.7-30.4
430(a3)	1.0	227-8	20	26	21	41.7-42.1(a3)	27.1-27.8
430(a4)	1.5	196-7	17	26	22	46.0-49.8(a4)	39.8-40.7
455(a4)	1.5	267-8	23	20	18	46.9-47.9(a4)	30.7-31.4
155G	All	Averages are (e)				18.6 ± 0.5	14.6 ± 0.5
250G	All	Averages are (e)				28.0 ± 2.6	22.1 ± 0.9
430G	All	Averages are (e)				42.8 ± 3.9	31.9 ± 3.3

(a) Reproducibility runs (a1 with a1, a2 with a2, etc.).
(b) Median value and usual ranges of viscosity are 22 ± 2 cp; for temperatures, 24 ± 2°C (liquid) and 19.5 ± 1.5° (air).
(c) For upper speed range.
(d) Run numbers for the lower speed range are 1 and 2 for each sequence number.
(e) Average of midpoint values of each range.

Table 1 also shows the very good agreement obtained between the film thickness determined by direct micrometer measurements and that calculated using Equation (1) and the measured flowrate. This agreement provides an independent check on both measurements and on film width, and is necessary (but not sufficient) to indicate good film uniformity.

The micrometer film thickness is determined by averaging three values taken during each run. This brass tip micrometer is centered and placed approximately 0.28 m above the slide-contact point near the belt. Sensitivity of the micrometer is about 1 micron. The volume flowrate is determined, at the beginning and end of each sequence, by placing a graduated cylinder after the rotameter and collecting a one-minute sample. Flowrate variations were often about 5% in a sequence of runs and are averaged.

The effect of belt speed on bead size was also studied, using photography. Consider a typical result with a larger bead, such as that with the more viscous paraffin oil of 1.0 mm gap and 405 ml/min, sequence 37. Figure 4 shows a side view of the 68 $mN \cdot s/m^2$ (68 cp) oil at four speeds, increasing from 18 to 28 m/min. This figure shows the substantial reduction in bead size which occurs at increasing speeds.

In order to test for the possible presence of vortices within the bead, several tracer study experiments were performed using fluid P. These are done by injecting a visible dye from a syringe into a relatively large bead at several locations, including the surfaces. Bead size is kept relatively large by setting flow rate high (395 ml/min) and belt speed low (20 m/min). Visual observation is facilitated by using the maximum gap space (2.0 mm). When the dye is added at any point within or on the bead, the dye immediately moves upwards out of the bead and into the film on the belt, thereby confirming the absence of vorticity within the bead.

EFFECT OF FLOWRATE AND GAP SIZE FOR GLYCERIN DATA

Using the method outlined above, fourteen sequences of runs were made with the glycerin solution (sets 14 to 27). The upper and lower speed limit results are shown in Table 2, together with the range of independent variables (flowrate and gap size) and the range of conditions (liquid viscosity and temperatures). Most of the results shown were obtained directly from research notebooks; they are not shown explicitly in thesis form.

First, consider the precision of the Table 2 data by noting the pairs of reproducibility sequences; these were made at two gaps (1.0 mm and 1.5 mm) and at all three flowrates. For example, the repeat runs are labeled "a1" at low flow, "a2" at moderate flow and "a3" and "a4" at high flow. The reproducibility is within a few percent for all but the triplicate (a2) sequences.

Another indication of precision is film thickness. Calculated film thicknesses (h_a) agrees closely with measured glycerin thicknesses for all 14 sequences and for the whole range of independent variables studied. The variations are small and of random size. Differences between the measured and calculated values range from plus to minus and from 1 to 13%, most within 10%, so that this glycerin data appears to be good, based on this thickness test.

Table 2 shows that the dependence of either the upper or the lower speed limit on gap size is almost negligible. Both speed limits increase with only the 0.1 or 0.2 power of gap size. In contrast to the lack of effect of a three-fold variation in gap size is a rather significant increase in both the upper and lower speed limits for a three-fold increase in volume flowrate. The effect of flowrate on speed limits is shown graphically in Figure 5, as three plots at constant gap size. The resulting slopes reveal that both speed limits increase with approximately the 0.8 power of flowrate. Another feature of Figure 5 is the display of an "operability window," outside of which uniform films have not been found to occur.

SPEED LIMIT RESULTS WITH HIGHER VISCOSITY OILS

Speed limit results for ten sets of paraffin oil runs (sets 28 to 37) and eight sets of motor oil mixture runs (sets 38 to 45) are shown in Table 3, based on the research notebooks of Faust (1975). As with the low viscosity glycerin, flowrate proved to be a far more significant variable than gap size in influencing the speed limits. Speed limits averaged over a four-fold gap size are also given for five different conditions.

Speed limit results for the two oils are not considered as precise as the glycerin results, because the calculated oil film thicknesses are smaller than the measured values. For the paraffin oil runs, calculated values are about 15 to 30% smaller; the 15% occurred with the small, 0.5 mm gaps and the 30% with large, 2.0 mm gaps. Even larger differences were noted with the more viscous (M) liquid. The reasons for these thickness differences are not well understood. However, they occurred only with the higher viscosity liquids.

With the oil runs, the film width decreased with increasing speeds, from about 10 to 20% wider than the

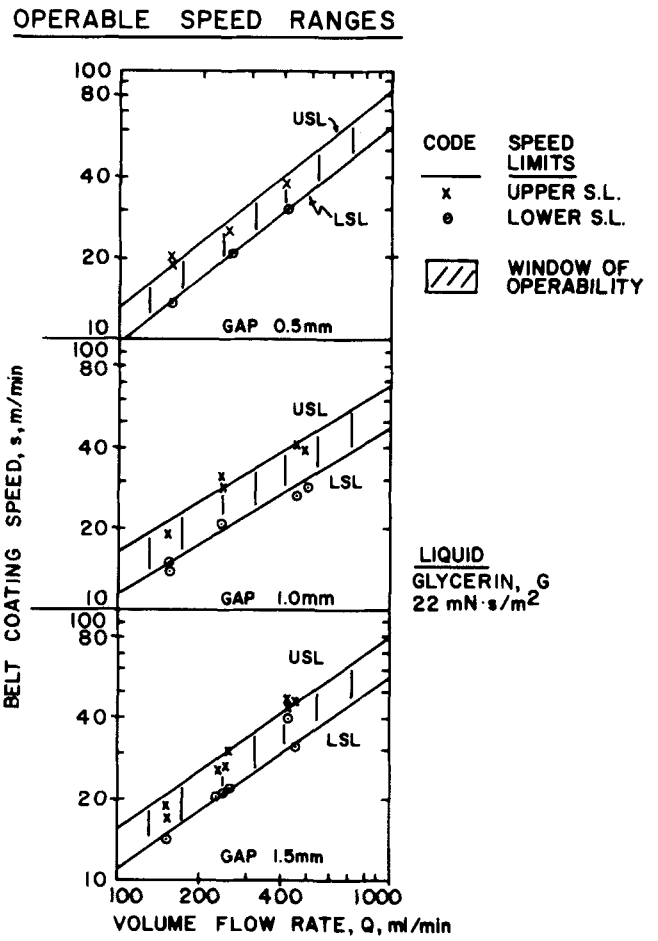

Figure 5. Operable ranges for the glycerin solution.

slide width at lower paraffin speeds, to about 10 to 20% narrower at higher speeds. This width-change behavior also affects the precision of the Table 3 speed limits to some extent, but the results are useful as a first approximation.

Despite the suspected lesser precision of these oil data, they show close agreement with the glycerin data in terms of the influence of flow rate and gap size on speed limits. Specifically, both speed limits increase with the 0.7 to 0.8 power of flowrate, compared to the 0.8 power with glycerin. Similarly, both speed limits increase with the 0.1 to 0.2 power of gap size, again the same as with glycerin.

EFFECT OF VISCOSITY ON SPEED LIMITS

As shown in Figure 6, increasing the liquid viscosity decreases both the upper and lower speed limits. The lower speed limits drop about 50% for a thirteen-fold increase in viscosity, and a similar decrease is observed for the upper speed limits. Thus both speed limits were proportional to viscosity raised, to about the minus 0.3 power. Figure 6 is drawn for the only gap size (0.5 mm) for which all three liquids were studied, but similar viscosity effects are found with the other gaps.

The effect of viscosity on the *size* of the operable speed range is unclear. Comparing the low and high viscosity liquids (glycerin and oil mixture), there appears to be a small decrease in range with increasing viscosity. However, the moderate viscosity results with paraffin oil do not follow that trend.

In summary, the primary influence on speed limit appears to be the volume flowrate (at about the 0.8 power) and the secondary influence is liquid viscosity (at about the minus 0.3 power), over the ranges we studied.

COMPARISON TO THE THEORY OF RUSCHAK

In an innovative theoretical analysis, Ruschak (1976) obtained predictive equations for the upper speed limit during bead coating. These equations are expressed in terms of two dimensionless groups: the Beguin number, *Be*, and the Lewis number, *Le*, defined as

$$Be = \frac{P_0 - P_b}{\rho g a} \tag{2}$$

$$Le = \frac{(\mu s/\sigma)}{(h_a/a)^{3/2}} = \frac{Ca}{H^{3/2}} \tag{3}$$

where a is capillary length, $(\sigma/\rho g)^{1/2}$, a property term, h_a is asymptotic film thickness, s is belt speed, Ca is the capillary number, $\mu s/\sigma$, and H is h_a/a. Here P_0 and P_b are the pressures above the top meniscus and below the lower meniscus, respectively. For stable conditions:

$$Be + \frac{a}{d}(1 + \cos\theta) \geqq 1.338\, Le^{2/3} \geqq Be - \frac{a}{d}(1 - \cos\theta) \tag{2a}$$

$$2\frac{a}{d} \geqq 1.338\, Le^{2/3} \tag{3a}$$

where θ is the static contact angle. These algebraic inequalities imply, for example, that a higher pressure above the upper meniscus (higher *Be*) leads to higher

TABLE 3. RUN CONDITIONS AND SPEED LIMITS FOR OIL SOLUTIONS P AND M

Flowrate Q, ml/min	Size of gap, mm	Run Nos. (c)	Liquid prop. air			Range of speed limits, m/min	
			μ, cp	T°C	T°C	Upper speed (split)	Lower speed (drip) (d)
164P	0.5	325-6	68	22	18	14.4-15.1	8.1-9.6
164P	1.0	335-6	68	24	19	13.4-14.8	9.6-10.1
162P	2.0	356-7	71	22	18	17.2-18.7	10.5-11.0
250P	0.5	305-6	66	22	19	18.2-20.6	11.7-12.5
258P	1.0	285-6	67	22	20	15.6-16.0	12.2-12.5
260P	2.0	345-6	70	21	18	21.1-23.5	15.3-15.8
402P	0.5	316-7	66	24	19	27.5-28.3	16.3-16.8
400P(a1)	1.0	296-7	68	24	19	26.1-27.1(a1)	15.8-16.8
407P(a1)	1.0	376-7	71	23	19	28.0-29.7(a1)	17.7-18.4
395P	2.0	366-7	69	21	19	28.0-28.8	18.7-19.4
165P	All	Averages are (e)				15.6 ± 1.8	9.9 ± 0.6
255P	All	Averages are (e)				19.2 ± 2.2	13.4 ± 1.5
400P	All	Averages are (e)				28.0 ± 0.7	17.5 ± 1.0
170M(a2)	0.5	417-8	307(b)	19	17	10.1-10.8(a2)	6.7-7.4
172M(a2)	0.5	426-7	281	21	18	10.5-11.0(a2)	6.7-7.4
165M(a3)	2.0	406-6	332(b)	19	16	8.4-8.6(a3)	6.7-7.2
176M(a3)	2.0	434-5	281	22	19	9.6-10.1(a3)	7.2-7.7
265M(a4)	0.5	387-8	230(b)	22	19	12.1-13.4(a4)	10.1-10.5
257M(a4)	0.5	455-6	281	22	18	11.5-12.0(a4)	9.6-10.5
245M(a5)	2.0	396-7	232(b)	24	21	12.0-13.2(a5)	9.6-10.5
257M(a5)	2.0	445-6	281	21	18	10.5-10.8(a5)	8.4-8.6
165M	All	Averages are (e)				9.9 ± 0.7	7.2 ± 0.2
255M	All	Averages are (e)				12.1 ± 0.8	9.8 ± 0.6

(a) Reproducibility runs (a1 with a1, a2 with a2, etc.).
(b) Except for these 4 runs, in which viscosity varied considerably, median value of viscosities were 68 and 281 cp.
(c) For upper speed range.
(d) Run numbers for the lower speed range are 1 and 2 for each sequence number.
(e) Average of midpoint values of each range.

stable belt speeds. In the present work, the pressure difference is zero, and thus Be is zero. For this case then, Equations (2a) and (3a) reduce to the single inequality condition

$$\frac{a}{d}(1+\cos\theta) \geq 1.338\, Le^{2/3} \qquad (4)$$

This theory therefore predicts only the upper speed limit, and not the lower. Ruschak (1976) indicates that his analysis represents only a first approximation to bead coating. An important limitation to the Ruschak theory is the assumption of a *static* lower meniscus. This rules out prediction of the "drip point," in which the liquid proceeds from the trough to drip down the moving belt. The contact angle θ is roughly zero for the fluids of this study so that Equation (4), after substituting Equation (1), leads to a quantitative prediction of the upper speed limit:

$$S_3 = \left[\frac{1.495Q}{bd}\right]^{3/5}\left[\frac{\sigma}{\mu}\right]^{2/5} \qquad (5)$$

With respect to the principle independent variables of this study, S_3 increases with flowrate Q and decreases with increasing gap spacing d and viscosity μ.

Equation (5) predicts that the upper speed limit, S_3, increases with flowrate, Q, raised to the 0.6 power. This exponent compares quite favorably with slopes from the glycerin data on Figure 5, which yields experimental exponents ranging from 0.7 to 0.8. For the two oil samples, Table 3 experimental values for this exponent (obtained for constant gap size and viscosity) also range from 0.7 to 0.8. In summary, therefore, Ruschak's theoretical prediction of the effect of flowrate on upper speed limit is in close agreement with our experimental data.

Ruschak's theory predicts that the upper speed limit decreases with increasing viscosity; this trend is also apparent from the experimental data of Figure 6. From Equation (5), S_3 is proportional to the -0.4 power of viscosity. By comparison, the slopes of Figure 6 are about -0.34 and the data in Tables 2 and 3 lead to an exponent of about -0.3. Considering the experimental difficulties and anomalous variations in film widths for the more viscous oils, this is rather good agreement between theory and experiment.

FURTHER COMPARISON OF UPPER LIMITS

Equation (5) predicts that the upper limit decreases with the 0.6 power of gap size, d. As noted earlier, the experimental data show little, if any, dependence of this speed limit on d. Of the three variables investigated, then, the influence of gap size is the only one which shows a marked difference between the Ruschak theory and our experiment. Whether this is a consequence of the approximations inherent in the theory or the experimental difficulty of maintaining *uniform* gap size at small values of d (0.5 mm) will be determined by further work.

In addition to predicting the influence of the several variables, Equation (5) predicts absolute values of the upper speed limit. In Table 4 these predicted values are compared with the experimental values, as functions of flowrate, gap size, and specific fluid. In all but three of the 27 pair comparisons, the predicted value is higher than the experimental. For the smallest gap size, 0.5 mm, the predicted values are two to three times as large as

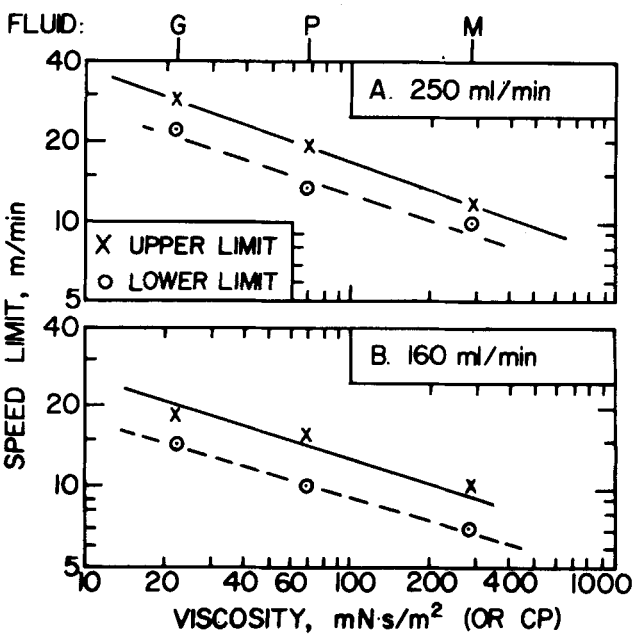

Figure 6. Effect of viscosity on operable speed limits.

TABLE 4. NUMERICAL COMPARISON OF UPPER SPEED LIMITS: EXPERIMENTAL DATA AND PREDICTIONS BY RUSCHAK THEORY

Fluids and flowrate	Upper speed limits (m/min)							
	Gap size 0.5 mm		Gap size 1.0 mm		Gap size 1.5 mm		Gap size 2.0 mm	
	Exp.	Pred.*	Exp.	Pred.*	Exp.	Pred.*	Exp.	Pred.*
G: Glycerin								
155 ml/min	20	63	18	42	18	33	—	—
250 ml/min	26	86	30	56	28	44	—	—
450 ml/min	38	122	41	81	48	63	—	—
P: Paraffin oil								
165 ml/min	15	36	14	24	—	—	18.0	15.8
255 ml/min	19	49	16	33	—	—	22.5	21.4
400 ml/min	28	65	28	43	—	—	28.4	28.4
M: Oil mixture								
170 ml/min	10.7	22.0	—	—	—	—	9.2	9.6
255 ml/min	12.5	28.1	—	—	—	—	11.6	12.2

* Predicted values of upper speed limits.

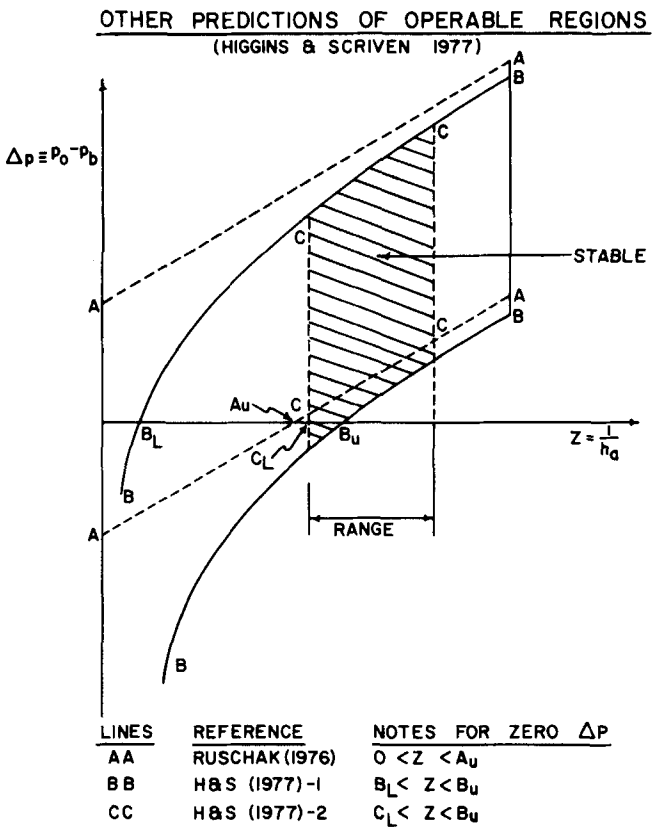

Figure 7. Theory of Ruschak (1976) and Higgins-Scriven (1977).

the experimental. However, the agreement improves considerably as gap size increases so that, for $d = 2.0$ mm, the agreement is within 10%. Even for the glycerin solution, it appears that the trend with d is such that, had experiments been conducted for a d of 2.0 mm (as for the two oils) instead of only 1.5 mm, close agreement would also be obtained for this solution. Of course, the anomalous effect of gap size in Table 4 is consistent with the discrepancy noted earlier for this particular variable. The effects of flow rate and viscosity (fluid type) in Table 4 exhibit the same approximate agreement between theory and experiment which was noted earlier for these particular variables.

In summary, it appears that Equation (5) is remarkably accurate in predicting the upper limit for the larger gap sizes, considering the approximations in the theory and the experimental variations. Moreover, Equation (5) provides approximately correct predictions of first, the effect of flowrate (0.8 power experimental versus 0.6 power predicted) and second, the effect of viscosity, (−0.3 power experimental versus −0.4 power). The effect of gap size requires further investigation.

DISCUSSION OF THE LOWER SPEED LIMIT

As shown above, the simple theory of Ruschak (1976) does not predict a lower speed limit for zero ΔP conditions. Consideration of other and more complex factors in the model, however, could lead to predictions of lower speed limits.

One such study is the work in progress by Higgins and Scriven (1977, 1978). Some of their results are given in Figure 7. Lines AA represent the Ruschak theory (1976), based on a quasi-static meniscus for the lower meniscus. Lines BB represent a second model (Higgins and Scriven 1977) which includes dynamic effects on the lower meniscus.

Figure 7 shows that the BB theory predicts a lower speed limit for the zero ΔP case, specifically that given by point B_L on the horizontal axis. The point B_u predicts some shift in the upper speed limit. The lines CC on Figure 7 represent a third model (Higgins and Scriven 1977) which considers other interfacial aspects not included in the first two models. This CC theory predicts the narrow window of operability shown. For the zero ΔP case, the CC theory also predicts a quite narrow range of speed limits, namely those indicated by axis points C_L and B_u. Comparing these new models with data would be of considerable interest. Publication of the new models is planned (Higgins and Scriven 1978).

ACKNOWLEDGMENT

Much of the experimental part of this work was supported by the Eastman Kodak Co., and we are grateful for this support.

NOTATION

a = capillary length, $(\sigma/\rho g)^{1/2}$, mm
b = width of coating support, mm
Be = Beguin number, $\Delta P/\rho g a$, dimensionless
Ca = Capillary number, $\mu s/\sigma$, dimensionless
d = gap size, distance between slide and support, mm
g = gravitational field, m/s^2
h = meniscus thickness from support, mm
h_a = .lm thickness, asymptotic, mm
H = .ilm thickness h_a/a, dimensionless
Le = Levich number, $Ca/H^{3/2}$, dimensionless
s = speed of support, m/min
S = upper speed limit, m/min
S_3 = upper speed limit, model, Equation (5)
Q = volume flowrate, ml/min
x = vertical coating coordinate, Figure 1
y = horizontal coating coordinate, Figure 1

Greek Symbols

α = angle between slide and normal to belt
μ = viscosity, mN·s/m^2
ρ = density, kg/m^3
σ = surface tension, N/km
θ = contact angle, static, solid-liquid

LITERATURE CITED

Beguin, Albert E., "Method of Coating Strip Material," U.S. Patent 2,681,294 (June 1954).

Gutfinger, Chaim, "Films of Non-Newtonian Fluids in Laminar Motion on Vertical Plates," Ph.D. Dissertation, Yale University, New Haven (1964).

Gutfinger, Chaim and J. A. Tallmadge, "Films of Non-Newtonian Fluids Adhering to Flat Plates," *AIChE J.*, **11**, 403 (1964).

Faust, Helen L., "Menisci Studies in Bead Coating," MS Thesis, Dept. of Chem. Eng., Drexel University, Philadelphia (1975).

Higgins, B. G. and L. E. Scriven, "Capillary Pressure and Viscous Pressure Drop Set Bounds on Coating Bead Operability," 70th Annual AIChE Mtg., New York (1977).

Higgins, B. G. and L. E. Scriven, personal communication (1978).

Ruschak, Kenneth J., "Limiting Flow in a Pre-Metered Coating Device," *Chem. Eng. Sci.*, 31, 1057 (1976).

Soroka, Anthony J., "Continuous Withdrawal of Newtonian Liquid Films on Vertical Plates," PhD Dissertation, Drexel University, Philadelphia (1969).

Tallmadge, J. A., C. B. Weinberger, and H. L. Faust, "Bead Coating Instability," 71st. Annual AIChE Mtg., Miami Beach (1978).

Manuscript received October 23, 1978; revision received April 11, and accepted June 15, 1979.